Long-term Responsivity Stability of ISOPHOT-S

Bernhard Schulz
ISO Data Centre, Astrophysics Division, ESA, Villafranca, Spain

28 May 1999

Abstract

The long-term responsivity stability of the low resolution spectrometer subsystem of ISOPHOT (PHT-S) is investigated. The assessment includes the variation of the two 64 pixel subarrays (SS and SL) w.r.t. each other. PHT-S staring observations of four celestial calibration standards that were measured several times during the ISO mission, have been evaluated using the dynamic calibration method [1]. The overall reproducibility of the integrated fluxes, summed over pixels 5 to 63 (SS) and 66 to 111 (SL) is found to be $\approx$ 10 %. Removal of a trend depending on orbital phase improves the result by only one percent. The relative variation between the two subarrays is found to be 6 %. The values apply for staring observations and represent an upper limit for chopped observations.

1 Introduction

The ISOPHOT subinstrument PHT-S is a mid infrared spectrometer with a mean spectral resolution of $(\frac{\lambda}{\Delta\lambda}) \approx 95$ [3]. It hosts two Si:Ga arrays of 64 pixels each: SS for λ = 2.5 - 5.5, SL for λ = 6.0 - 11.6 μm.

The internal reference source (FCS) is not used in PHT-S observations for flux calibration, since it is not possible to sufficiently illuminate the short wavelength array without saturating the long wavelength array. For the standard OLP calibration it is assumed that the average detector responsivity along the orbit and from orbit to orbit is constant.

Correction for short term signal transients is available for staring observations (dynamic calibration). The method uses a library of signal transient curves measured on calibration stars for each pixel over the full range of accessible fluxes [1]. Short term transients in chopped PHT-S observations are corrected using a specific average response function for this observing mode and a subsequent correction depending on the signal difference between the chopper plateaux [2].

To test the assumption of a constant average responsivity in order to support programs e.g. monitoring variability of astronomical sources with PHT-S, the reproducibility of the measurements and thus the stability of the instrument was investigated. In the following we will use both terms, reproducibility and stability in the same sense.

2 Observations

The ISO database was searched for measurements of calibration sources with similar measurement set-up, that were repeated many times. We found suitable datasets for 4 standard stars. The flux densities of the targets at 2.5 μm ranged between 17 and 1500 Jy. For the chopped mode no adequate dataset was found.

The observations were performed on the standard stars HR6705 (γ-Dra), HR6688, HR5986 and HR6817. The measurement times ranged between 64 and 1024 s with the majority at 128 s. In some cases different reset intervals of the integration ramps were used for the same source, however the analysis showed no significant effects by these differences in the measurement setup. A summary of TDT numbers, measurement times and reset interval lengths is given in Table 2.

3 Data Processing and Results

All ERD-data were processed to SRD-level in a standard way using PIA V7.3.2(e) [4]. Some deviations from the default settings were chosen, in order to improve the results: i) Instead of the standard de-glitching at ramp-level, 2-level de-glitching with default parameters was used. ii) The first readout of each ramp was always de-selected. iii) The ramps of 128 readouts were subdivided into 16 subramps before slope fitting. iv) The de-glitching parameters at signal-level (SRD) were improved, e.g. the repetition factor was set to 5, the local distribution was set to 12 and Minimum/Maximum-clipping was selected. v) The time dependent dark signal was subtracted for each signal individually.

At SRD level the dynamic calibration was used, to directly obtain flux densities and to produce AAP-results. The number of calibration standards used for the dynamic calibration was between 2 and 3 and weighting by signal ratio was used.

The final AAP-results of all on-source measurements were further processed in proper IDL-procedures. For some observations no background observations were available, however they could be neglected because of the sufficient contrast between source and background flux levels. Even for the faintest source HR6817 the SED falls not below 1.5 Jy at the longest wavelength.

For each pixel all fluxes measured on the same source were normalised to the average flux of that pixel. The resulting normalised spectra are plotted in Figs. 1 to 4. The scatter is a measure for the reproducibility of the PHT-S detectors. It clearly varies along the arrays. To determine the overall stability of the PHT-S

Object	SS	SL	SS-SL	n	ϱ
HR6705	5.3	5.7	8.4	22	-0.17
HR6688	10.4	10.3	4.9	17	0.46
HR5986	14.4	14.7	1.6	7	0.99
HR6817	10.7	15.9	6.8	16	0.98
All	9.3	11.1	6.5		

Table 1: The r.m.s. values of the scatter of the normalised signals (column 2 & 3) and the relative variation between the subarrays SS and SL (column 4) determined from repeated measurements of four calibration standards. Column 5 shows the number of measurements (n) used and column 6 gives the correlation coefficients ϱ between SS and SL. All other values are per cent.

arrays, the averages of pixels 5 to 63 for SS and 66 to 111 for SL were calculated for each spectrum [1]. The scatter for each array, expressed in r.m.s values, is given in Table 1. The objects are ordered in decreasing brightness from top to bottom. The bottom row in the table gives the overall r.m.s values.

Fig. 5 to 8 show the array averages of the normalised spectra of SS and SL against the orbital phase. The orbital phase is the time within a revolution, starting at perigee, normalised to the time of a full revolution. The three brighter objects (HR6705, HR6688 and HR5986) show a falling trend along the revolution. Removal of this trend by a second order polynomial however reduces the r.m.s. scatter for all objects only slightly to 8.7 and 10.2 % for SS and SL respectively. The values in Table 1 are calculated from the uncorrected data.

Comparing the normalised signals of both arrays at the same time, we find that the responsivity variations in both arrays are correlated, if the amplitude of the variations exceeds 10 %. The differences of the normalised averages between arrays SS and SL are another measure of how well the variation in the average responsivities of both arrays correspond to each other. Table 1 summarises these differences as r.m.s. values in per cent and also shows the correlation coefficients between SS and SL. The mean difference is 6.5$\pm$2.5 % and is significantly smaller than the variations of each array separately, except for HR6705, where already the separate variations were small. For at least part of the variations, this points towards a common source affecting both arrays. Changes in the cosmic particle flux and in the temperature of the optical support structure (OSS) are likely explanations.

[1] The actual selection of the pixels originates from the scientific program this investigation was initiated by. However the ranges should still represent well the full detector arrays.

TDT	t_{meas} [s]	t_{reset} [s]	TDT	t_{meas} [s]	t_{reset} [s]
HR6705			HR6688		
04102802-00	128	0.125	02501103-01	128	1.0
05700504-01	128	0.125	02502503-01	128	1.0
05701404-01	256	0.125	02503303-01	128	1.0
05702304-01	256	0.125	02503903-01	128	1.0
05703404-01	128	0.125	05700403-01	128	1.0
05704704-01	128	0.125	05701303-01	128	1.0
07401401-01	128	0.125	05702203-01	128	1.0
23000802-00	128	0.125	05703303-01	128	1.0
28600302-00	128	0.125	05704603-01	128	1.0
28602902-00	128	0.125	08600202-00	128	1.0
28603802-00	128	0.125	08605002-00	128	1.0
28604802-00	128	0.125	09300202-00	128	1.0
28605602-00	128	0.125	09304302-00	128	1.0
34203113-00	128	0.125	23700402-00	128	1.0
34204931-00	128	0.125	31404802-00	256	4.0
34206850-00	128	0.125	39800402-01	256	1.0
34208668-00	256	0.125			
37000302-00	256	0.125			
37001102-00	256	0.125			
37003002-00	256	0.125			
37003902-00	256	0.125			
37006002-00	256	0.125			
HR5986			HR6817		
07709402-00	256	16.0	05701202-01	128	16.0
37700602-00	256	4.0	05702102-01	128	16.0
37700804-00	256	4.0	05703202-01	128	16.0
41901502-00	512	8.0	05703501-01	128	16.0
49603702-00	512	8.0	05703501-02	128	16.0
52401702-01	512	8.0	05703501-03	128	16.0
52401801-01	512	8.0	05703501-04	128	16.0
			05703501-05	128	16.0
			05704502-01	1024	32.0
			05704801-01	512	16.0
			05704801-02	256	8.0
			05704801-03	128	4.0
			05704801-04	64	2.0
			05704801-05	1024	32.0
			05704901-00	512	16.0
			74801402-01	64	2.0

Table 2: The measurements used for this analysis. The columns show TDT-number, duration of the measurement and reset interval used respectively.

4 Discussion

On average we find 10 % for the overall stability of PHT-S, with 9 % for SS and 11% for SL (see Table 1). However the values vary considerably for the individual objects. For the brightest source (HR6705) we find quite small variations of about 6 % even though the transient fitting for this source was poorest. The three brightest sources show no significant difference between the variations found for both arrays, although they differ by about a factor of 5 in average flux. Only the faintest star HR6817 shows a larger difference between SS and SL. Fig. 4 suggests that another noise component starts to dominate at low flux levels.

Part of the flux variations between measurements are introduced by transients coupled with different measurement times. These variations can to a large extent be eliminated by applying the dynamic calibration for PHT-S staring observations. This worked best for HR5986 and worst for HR6705. The quality of the transient fit is influenced by the detector temperature, which went outside nominal boundaries in many cases but was ignored here. The effect however seems to be small in view of the poor quality of the transient fits that was achieved at high fluxes in general. In particular pixels 1-12 (see Fig. 1) did not degrade the r.m.s. value for the SS array.

The stability figures, found in this analysis, primarily apply for normal staring mode observations. Unfortunately no sufficiently large data set of chopped PHT-S observations on a non-variable source could be found in the database. Although chopped mode observations can show strong transients, these are repeated in the same way during each chopper cycle and represent a very reproducible pattern for the same measurement setup. Also long-term drifts of the dark current are better eliminated than for staring mode observations. If the scatter in staring measurements is not only due to responsivity variations but also due to i) imperfect transient fitting, ii) variations of the background and/or iii) variations of the dark signal, then the reproducibility of chopped measurements should be better than the 10 % found here.

Acknowledgement: The Author thanks Rene Laureijs for his valuable suggestions.

References

[1] Acosta-Pulido, J.A. 1999, in preparation

[2] Acosta-Pulido, J.A. 1998, technical report, ISO Data Centre, VILSPA, `www.iso.vilspa.esa.es/users/expl_lib/PHT/chop_report02.ps.gz`

[3] Klaas, U., Acosta-Pulido, J.A., et al. 1997, ESA SP-419

[4] Gabriel, C., et al, 1997, ASP Conf.Ser., Vol.125, eds. G. Hunt & H.E. Payne, p108

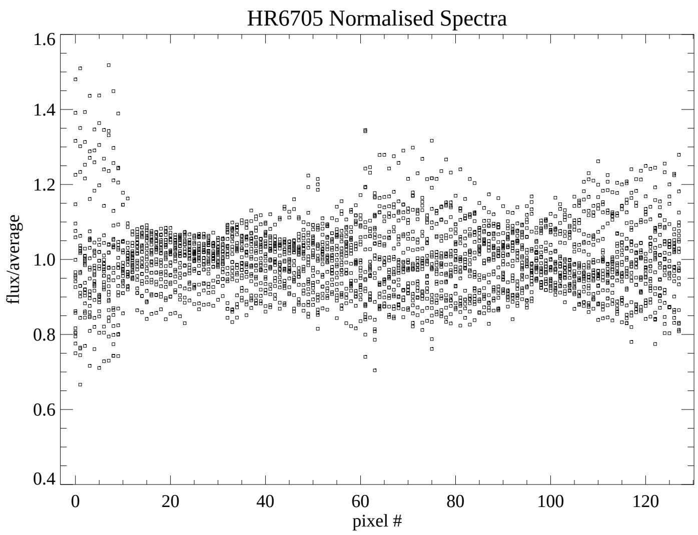

Figure 1: Signals of various γ-Dra observations, normalised to their mean value individually for each pixel. The scatter shows the reproducibility of the results in various parts of the arrays. Pixels 1-64 correspond to array SS, 65-128 belong to SL.

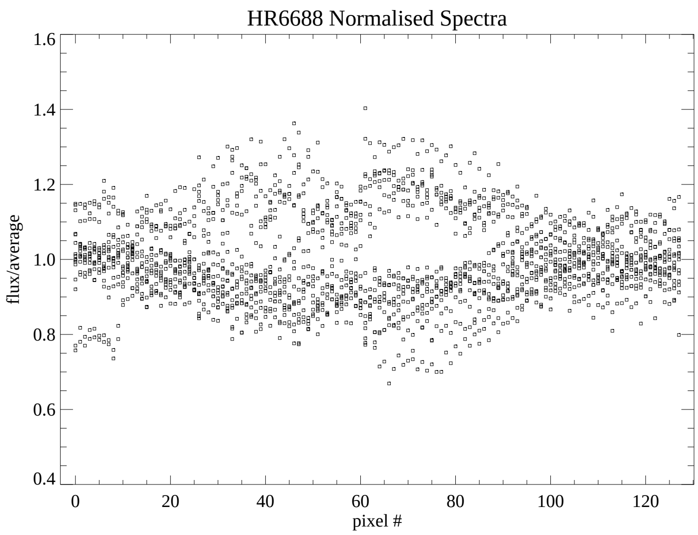

Figure 2: Signals of various HR6688 observations, normalised to their mean value individually for each pixel. The scatter shows the reproducibility of the results in various parts of the arrays. Pixels 1-64 correspond to array SS, 65-128 belong to SL.

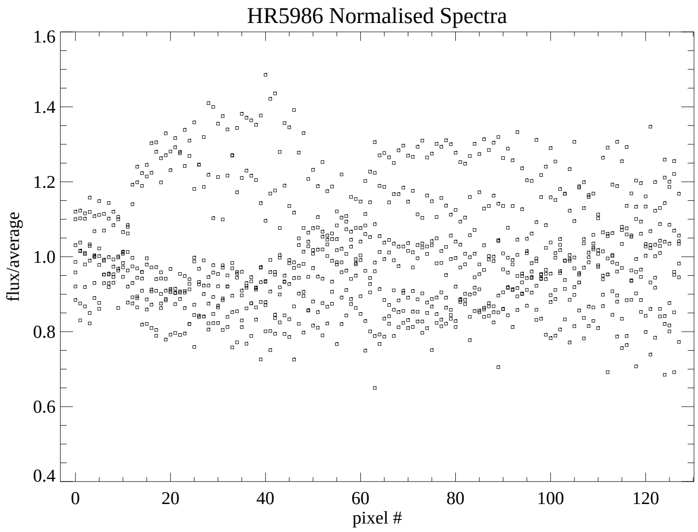

Figure 3: Signals of various HR5986 observations, normalised to their mean value individually for each pixel. The scatter shows the reproducibility of the results in various parts of the arrays. Pixels 1-64 correspond to array SS, 65-128 belong to SL.

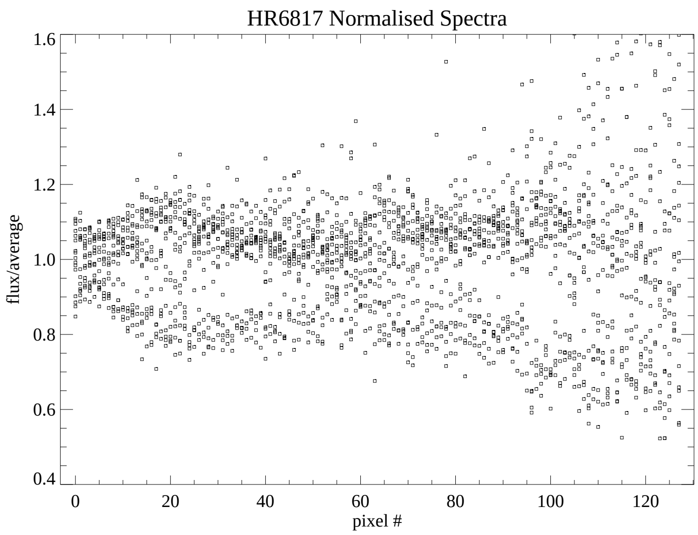

Figure 4: Signals of various HR6817 observations, normalised to their mean value individually for each pixel. The scatter shows the reproducibility of the results in various parts of the arrays. Pixels 1-64 correspond to array SS, 65-128 belong to SL.

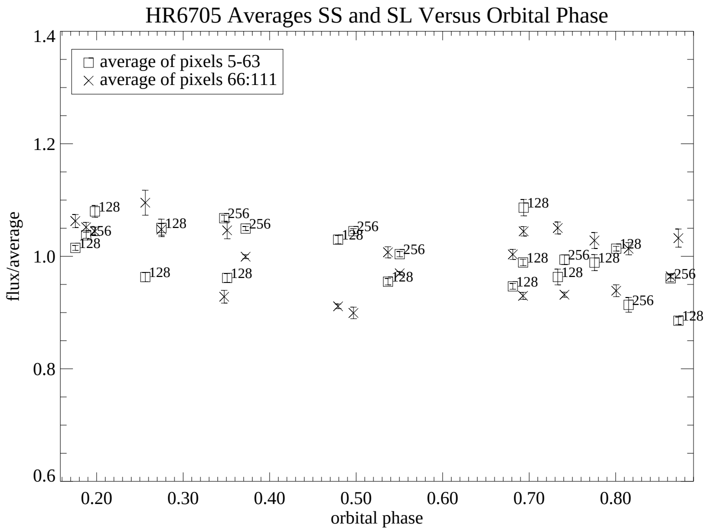

Figure 5: HR6705: The averages of pixels 5 to 63 and 66 to 111 plotted versus orbital phase.

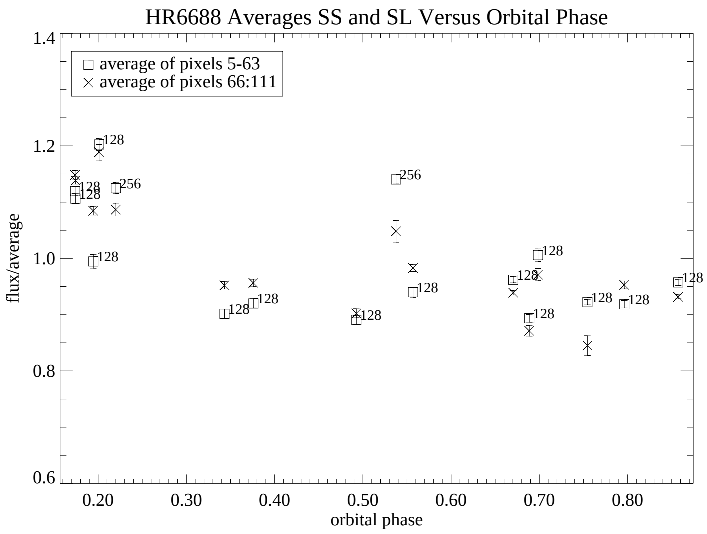

Figure 6: HR6688: The averages of pixels 5 to 63 and 66 to 111 plotted versus orbital phase.

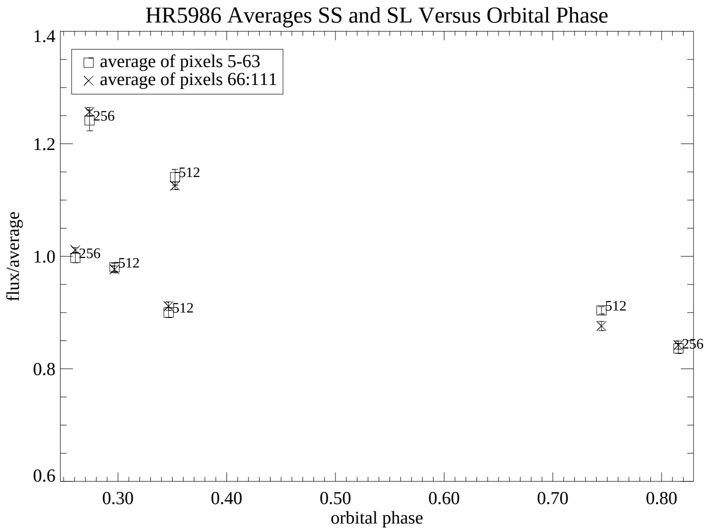

Figure 7: HR5986: The averages of pixels 5 to 63 and 66 to 111 plotted versus orbital phase.

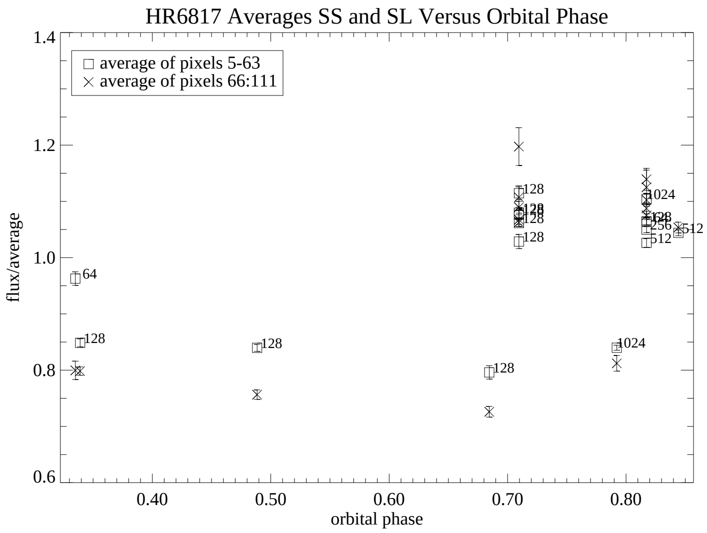

Figure 8: HR6817: The averages of pixels 5 to 63 and 66 to 111 plotted versus orbital phase.